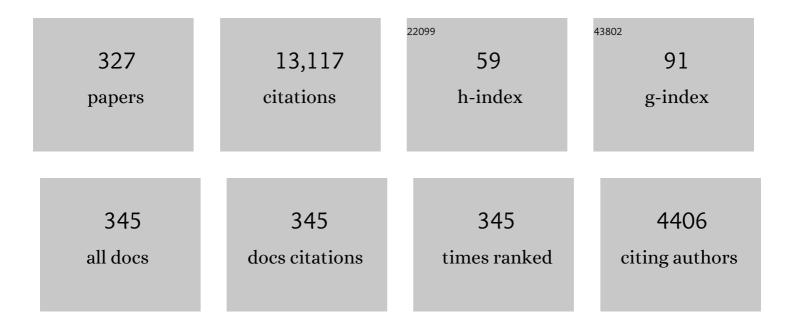
List of Publications by Year in descending order

Source: https://exaly.com/author-pdf/6494504/publications.pdf Version: 2024-02-01



#	Article	IF	CITATIONS
1	Discrete Aurora at Mars: Dependence on Upstream Solar Wind Conditions. Journal of Geophysical Research: Space Physics, 2022, 127, .	0.8	7
2	Observations and Modeling of Martian Auroras. Space Science Reviews, 2022, 218, .	3.7	1
3	Density and Temperature of the Upper Mesosphere and Lower Thermosphere of Mars Retrieved From the OI 557.7Ânm Dayglow Measured by TGO/NOMAD. Journal of Geophysical Research E: Planets, 2022, 127, .	1.5	6
4	The Mars Oxygen Visible Dayglow: A Martian Year of NOMAD/UVIS Observations. Journal of Geophysical Research E: Planets, 2022, 127, .	1.5	2
5	Planetâ€Wide Ozone Destruction in the Middle Atmosphere on Mars During Global Dust Storm. Geophysical Research Letters, 2022, 49, .	1.5	7
6	Laboratory Study of the Cameron Bands, the First Negative Bands, and Fourth Positive Bands in the Middle Ultraviolet 180–280Ânm by Electron Impact Upon CO. Journal of Geophysical Research E: Planets, 2021, 126, .	1.5	7
7	Morphology of Jupiter's Polar Auroral Bright Spot Emissions via Junoâ€UVS Observations. Journal of Geophysical Research: Space Physics, 2021, 126, e2020JA028586.	0.8	5
8	Are Dawn Storms Jupiter's Auroral Substorms?. AGU Advances, 2021, 2, e2020AV000275.	2.3	25
9	Detection of a Bolide in Jupiter's Atmosphere With Juno UVS. Geophysical Research Letters, 2021, 48, e2020GL091797.	1.5	9
10	Variability and Hemispheric Symmetry of the Pedersen Conductance in the Jovian Aurora. Journal of Geophysical Research: Space Physics, 2021, 126, e2020JA028949.	0.8	1
11	Detection and Characterization of Circular Expanding UVâ€Emissions Observed in Jupiter's Polar Auroral Regions. Journal of Geophysical Research: Space Physics, 2021, 126, e2020JA028971.	0.8	4
12	First Observation of the Oxygen 630Ânm Emission in the Martian Dayglow. Geophysical Research Letters, 2021, 48, e2020GL092334.	1.5	8
13	Discrete Aurora on Mars: Spectral Properties, Vertical Profiles, and Electron Energies. Journal of Geophysical Research: Space Physics, 2021, 126, e2021JA029495.	0.8	12
14	A Preliminary Study of Magnetosphereâ€lonosphereâ€Thermosphere Coupling at Jupiter: Juno Multiâ€Instrument Measurements and Modeling Tools. Journal of Geophysical Research: Space Physics, 2021, 126, e2021JA029469.	0.8	11
15	Discrete Aurora on Mars: Insights Into Their Distribution and Activity From MAVEN/IUVS Observations. Journal of Geophysical Research: Space Physics, 2021, 126, e2021JA029428.	0.8	20
16	First ICONâ€FUV Nighttime NmF2 and hmF2 Comparison to Ground and Spaceâ€Based Measurements. Journal of Geophysical Research: Space Physics, 2021, 126, e2021JA029360.	0.8	11
17	Local Time Dependence of Jupiter's Polar Auroral Emissions Observed by Juno UVS. Journal of Geophysical Research E: Planets, 2021, 126, e2021JE006954.	1.5	9
18	Imaging of Martian Circulation Patterns and Atmospheric Tides Through MAVEN/IUVS Nightglow Observations. Journal of Geophysical Research: Space Physics, 2020, 125, e2019JA027318.	0.8	13

#	Article	IF	CITATIONS
19	Possible Transient Luminous Events Observed in Jupiter's Upper Atmosphere. Journal of Geophysical Research E: Planets, 2020, 125, e2020JE006659.	1.5	13
20	Spatial Distribution of the Pedersen Conductance in the Jovian Aurora From Junoâ€UVS Spectral Images. Journal of Geophysical Research: Space Physics, 2020, 125, e2020JA028142.	0.8	19
21	Isobar Altitude Variations in the Upper Mesosphere Observed With IUVSâ€MAVEN in Response to Martian Dust Storms. Geophysical Research Letters, 2020, 47, e2020GL087468.	1.5	4
22	Detection of green line emission in the dayside atmosphere of Mars from NOMAD-TGO observations. Nature Astronomy, 2020, 4, 1049-1052.	4.2	13
23	Airglow remote sensing of the seasonal variation of the Martian upper atmosphere: MAVEN limb observations and model comparison. Icarus, 2020, 341, 113666.	1.1	11
24	A Longâ€Lasting Auroral Spiral Rotating Around Saturn's Pole. Geophysical Research Letters, 2020, 47, e2020GL088810.	1.5	4
25	Junoâ€UVS Observation of the Io Footprint During Solar Eclipse. Journal of Geophysical Research: Space Physics, 2019, 124, 5184-5199.	0.8	19
26	MAVENâ€IUVS Observations of the CO ₂ ⁺ UV Doublet and CO Cameron Bands in the Martian Thermosphere: Aeronomy, Seasonal, and Latitudinal Distribution. Journal of Geophysical Research: Space Physics, 2019, 124, 5816-5827.	0.8	18
27	Cassini UVIS Detection of Saturn's North Polar Hexagon in the Grand Finale Orbits. Journal of Geophysical Research E: Planets, 2019, 124, 1979-1988.	1.5	5
28	Auroral Beads at Saturn and the Driving Mechanism: Cassini Proximal Orbits. Astrophysical Journal Letters, 2019, 885, L16.	3.0	10
29	On the Relation Between Jovian Aurorae and the Loading/Unloading of the Magnetic Flux: Simultaneous Measurements From Juno, Hubble Space Telescope, and Hisaki. Geophysical Research Letters, 2019, 46, 11632-11641.	1.5	32
30	The Olâ€135.6Ânm Nighttime Emission in ICONâ€FUV Images: A New Tool for the Observation of Classical Mediumâ€Scale Traveling Ionospheric Disturbances?. Journal of Geophysical Research: Space Physics, 2019, 124, 7670-7686.	0.8	2
31	Kinetic Monte Carlo Model for the Precipitation of High-Energy Protons and Hydrogen Atoms into the Atmosphere of Mars with Taking into Account the Measured Magnetic Field. Astronomy Reports, 2019, 63, 835-845.	0.2	12
32	H3+ characteristics in the Jupiter atmosphere as observed at limb with Juno/JIRAM. Icarus, 2019, 329, 132-139.	1.1	11
33	Characteristics of Mars UV Dayglow Emissions From Atomic Oxygen at 130.4 and 135.6 nm: MAVEN/IUVS Limb Observations and Modeling. Journal of Geophysical Research: Space Physics, 2019, 124, 4809-4832.	0.8	12
34	UV Study of the Fourth Positive Band System of CO and O <scp>i</scp> 135.6Ânm From Electron Impact on CO and CO ₂ . Journal of Geophysical Research: Space Physics, 2019, 124, 2954-2977.	0.8	12
35	No detection of methane on Mars from early ExoMars Trace Gas Orbiter observations. Nature, 2019, 568, 517-520.	13.7	111
36	Martian dust storm impact on atmospheric H2O and D/H observed by ExoMars Trace Gas Orbiter. Nature, 2019, 568, 521-525.	13.7	107

#	Article	IF	CITATIONS
37	In-flight Characterization and Calibration of the Juno-ultraviolet Spectrograph (Juno-UVS). Astronomical Journal, 2019, 157, 90.	1.9	18
38	Contemporaneous Observations of Jovian Energetic Auroral Electrons and Ultraviolet Emissions by the Juno Spacecraft. Journal of Geophysical Research: Space Physics, 2019, 124, 8298-8317.	0.8	22
39	Lyman-α emission in the Martian proton aurora: Line profile and role of horizontal induced magnetic field. Icarus, 2019, 321, 266-271.	1.1	17
40	The Atmospheric Chemistry Suite (ACS) of Three Spectrometers for the ExoMars 2016 Trace Gas Orbiter. Space Science Reviews, 2018, 214, 1.	3.7	119
41	Investigations of the Mars Upper Atmosphere with ExoMars Trace Gas Orbiter. Space Science Reviews, 2018, 214, 1.	3.7	13
42	Jupiter's Aurora Observed With HST During Juno Orbits 3 to 7. Journal of Geophysical Research: Space Physics, 2018, 123, 3299-3319.	0.8	53
43	Temperature estimation from hydroxyl airglow emission in the Venus night side mesosphere. Icarus, 2018, 300, 386-391.	1.1	1
44	The Ionospheric Connection Explorer Mission: Mission Goals and Design. Space Science Reviews, 2018, 214, 1.	3.7	152
45	<i>Bar Code</i> Events in the Junoâ€UVS Data: Signature â^1⁄410ÂMeV Electron Microbursts at Jupiter. Geophysical Research Letters, 2018, 45, 12,108.	1.5	14
46	The O(¹ S) 297.2â€nm Dayglow Emission: A Tracer of CO ₂ Density Variations in the Martian Lower Thermosphere. Journal of Geophysical Research E: Planets, 2018, 123, 3119-3132.	1.5	14
47	Hubble Space Telescope Observations of Variations in Ganymede's Oxygen Atmosphere and Aurora. Journal of Geophysical Research: Space Physics, 2018, 123, 3777-3793.	0.8	16
48	Auroral Storm and Polar Arcs at Saturn—Final Cassini/UVIS Auroral Observations. Geophysical Research Letters, 2018, 45, 6832-6842.	1.5	10
49	A chemical survey of exoplanets with ARIEL. Experimental Astronomy, 2018, 46, 135-209.	1.6	249
50	The Largest Electron Differential Energy Flux Observed at Mars by the Mars Express Spacecraft, 2004-2016. Journal of Geophysical Research: Space Physics, 2018, 123, 6576-6590.	0.8	0
51	Recurrent Magnetic Dipolarization at Saturn: Revealed by Cassini. Journal of Geophysical Research: Space Physics, 2018, 123, 8502-8517.	0.8	14
52	NOMAD, an Integrated Suite of Three Spectrometers for the ExoMars Trace Gas Mission: Technical Description, Science Objectives and Expected Performance. Space Science Reviews, 2018, 214, 1.	3.7	95
53	Concurrent ultraviolet and infrared observations of the north Jovian aurora during Juno's first perijove. Icarus, 2018, 312, 145-156.	1.1	18
54	Juno observations of spot structures and a split tail in Io-induced aurorae on Jupiter. Science, 2018, 361, 774-777.	6.0	53

#	Article	IF	CITATIONS
55	Monte Carlo Simulations of the Interaction of Fast Proton and Hydrogen Atoms With the Martian Atmosphere and Comparison With In Situ Measurements. Journal of Geophysical Research: Space Physics, 2018, 123, 5850-5861.	0.8	15
56	Observations of the Proton Aurora on Mars With SPICAM on Board Mars Express. Geophysical Research Letters, 2018, 45, 612-619.	1.5	32
57	Evidence for Auroral Emissions From Callisto's Footprint in HST UV Images. Journal of Geophysical Research: Space Physics, 2018, 123, 364-373.	0.8	23
58	In-flight characterization and calibration of the Juno-Ultraviolet Spectrograph (Juno-UVS). , 2018, , .		2
59	Similarity of the Jovian satellite footprints: Spots multiplicity and dynamics. Icarus, 2017, 292, 208-217.	1.1	23
60	The Mars diffuse aurora: A model of ultraviolet and visible emissions. Icarus, 2017, 288, 284-294.	1.1	20
61	The thermal structure of the Venus atmosphere: Intercomparison of Venus Express and ground based observations of vertical temperature and density profiles. Icarus, 2017, 294, 124-155.	1.1	34
62	Jupiter's magnetosphere and aurorae observed by the Juno spacecraft during its first polar orbits. Science, 2017, 356, 826-832.	6.0	109
63	Infrared observations of Jovian aurora from Juno's first orbits: Main oval and satellite footprints. Geophysical Research Letters, 2017, 44, 5308-5316.	1.5	30
64	Preliminary JIRAM results from Juno polar observations: 2. Analysis of the Jupiter southern H ₃ ⁺ emissions and comparison with the north aurora. Geophysical Research Letters, 2017, 44, 4633-4640.	1.5	20
65	Preliminary JIRAM results from Juno polar observations: 1. Methodology and analysis applied to the Jovian northern polar region. Geophysical Research Letters, 2017, 44, 4625-4632.	1.5	18
66	Response of Jupiter's auroras to conditions in the interplanetary medium as measured by the Hubble Space Telescope and Juno. Geophysical Research Letters, 2017, 44, 7643-7652.	1.5	68
67	Morphology of the UV aurorae Jupiter during Juno's first perijove observations. Geophysical Research Letters, 2017, 44, 4463-4471.	1.5	54
68	Junoâ€UVS approach observations of Jupiter's auroras. Geophysical Research Letters, 2017, 44, 7668-7675.	1.5	25
69	Preliminary JIRAM results from Juno polar observations: 3. Evidence of diffuse methane presence in the Jupiter auroral regions. Geophysical Research Letters, 2017, 44, 4641-4648.	1.5	13
70	Nitric oxide nightglow and Martian mesospheric circulation from MAVEN/IUVS observations and LMDâ€MGCM predictions. Journal of Geophysical Research: Space Physics, 2017, 122, 5782-5797.	0.8	36
71	Changes in the Martian atmosphere induced by auroral electron precipitation. Solar System Research, 2017, 51, 362-372.	0.3	2
72	SPICAM on Mars Express: A 10 year in-depth survey of the Martian atmosphere. Icarus, 2017, 297, 195-216.	1.1	64

#	Article	IF	CITATIONS
73	The tails of the satellite auroral footprints at Jupiter. Journal of Geophysical Research: Space Physics, 2017, 122, 7985-7996.	0.8	57
74	Influence of the crustal magnetic field on the Mars aurora electron flux and UV brightness. Icarus, 2017, 282, 127-135.	1.1	17
75	Stagnation of Saturn's auroral emission at noon. Journal of Geophysical Research: Space Physics, 2017, 122, 6078-6087.	0.8	7
76	Mechanisms of Saturn's Nearâ€Noon Transient Aurora: In Situ Evidence From Cassini Measurements. Geophysical Research Letters, 2017, 44, 11,217.	1.5	10
77	Aeronomy of the Venus Upper Atmosphere. Space Science Reviews, 2017, 212, 1617-1683.	3.7	33
78	Corotating Magnetic Reconnection Site in Saturn's Magnetosphere. Astrophysical Journal Letters, 2017, 846, L25.	3.0	23
79	Dawn Auroral Breakup at Saturn Initiated by Auroral Arcs: UVIS/Cassini Beginning of Grand Finale Phase. Journal of Geophysical Research: Space Physics, 2017, 122, 12,111.	0.8	8
80	The Ultraviolet Spectrograph on NASA's Juno Mission. Space Science Reviews, 2017, 213, 447-473.	3.7	109
81	Magnetic reconnection during steady magnetospheric convection and other magnetospheric modes. Annales Geophysicae, 2017, 35, 505-524.	0.6	6
82	Pulsations of the polar cusp aurora at Saturn. Journal of Geophysical Research: Space Physics, 2016, 121, 11,952.	0.8	13
83	The color ratio-intensity relation in the Jovian aurora: Hubble observations of auroral components. Planetary and Space Science, 2016, 131, 14-23.	0.9	13
84	Analytical estimate for lowâ€altitude ENA emissivity. Journal of Geophysical Research: Space Physics, 2016, 121, 1167-1191.	0.8	9
85	Dynamics of the flares in the active polar region of Jupiter. Geophysical Research Letters, 2016, 43, 11,963.	1.5	19
86	SPICAM observations and modeling of Mars aurorae. Icarus, 2016, 264, 398-406.	1.1	52
87	Scientific problems addressed by the Spektr-UV space project (world space Observatory—Ultraviolet). Astronomy Reports, 2016, 60, 1-42.	0.2	63
88	A multi-scale magnetotail reconnection event at Saturn and associated flows: Cassini/UVIS observations. Icarus, 2016, 263, 75-82.	1.1	21
89	Concurrent observations of ultraviolet aurora and energetic electron precipitation with Mars Express. Journal of Geophysical Research: Space Physics, 2015, 120, 6749-6765.	0.8	37
90	Ten years of Martian nitric oxide nightglow observations. Geophysical Research Letters, 2015, 42, 720-725.	1.5	29

#	Article	IF	CITATIONS
91	Nonthermal radiative transfer of oxygen 98.9 nm ultraviolet emission: Solving an old mystery. Journal of Geophysical Research: Space Physics, 2015, 120, 10,772.	0.8	3
92	Auroral spirals at Saturn. Journal of Geophysical Research: Space Physics, 2015, 120, 8633-8643.	0.8	9
93	The EChO science case. Experimental Astronomy, 2015, 40, 329-391.	1.6	31
94	Terrestrial <scp>OH</scp> nightglow measurements during the <scp>Rosetta</scp> flyby. Geophysical Research Letters, 2015, 42, 5670-5677.	1.5	7
95	The far-ultraviolet main auroral emission at Jupiter – Part 1: Dawn–dusk brightness asymmetries. Annales Geophysicae, 2015, 33, 1203-1209.	0.6	22
96	The far-ultraviolet main auroral emission at Jupiter – Part 2: Vertical emission profile. Annales Geophysicae, 2015, 33, 1211-1219.	0.6	12
97	MONTE CARLO SIMULATION OF METASTABLE OXYGEN PHOTOCHEMISTRY IN COMETARY ATMOSPHERES. Astrophysical Journal, 2015, 798, 21.	1.6	5
98	Is the O2(a1Δg) Venus nightglow emission controlled by solar activity?. Icarus, 2015, 262, 170-172.	1.1	22
99	Science objectives and performances of NOMAD, a spectrometer suite for the ExoMars TGO mission. Planetary and Space Science, 2015, 119, 233-249.	0.9	77
100	Mars thermospheric scale height: CO Cameron and CO2+ dayglow observations from Mars Express. Icarus, 2015, 245, 295-305.	1.1	29
101	Saturn's elusive nightside polar arc. Geophysical Research Letters, 2014, 41, 6321-6328.	1.5	15
102	Jupiter's equatorward auroral features: Possible signatures of magnetospheric injections. Journal of Geophysical Research: Space Physics, 2014, 119, 10,068.	0.8	35
103	Dynamic auroral storms on Saturn as observed by the Hubble Space Telescope. Geophysical Research Letters, 2014, 41, 3323-3330.	1.5	43
104	Time variations of O2(a1î") nightglow spots on the Venus nightside and dynamics of the upper mesosphere. Icarus, 2014, 237, 306-314.	1.1	17
105	Isolating auroral FUV emission lines using compact, broadband instrumentation. Planetary and Space Science, 2014, 103, 291-298.	0.9	1
106	Latitudinal structure of the Venus O2 infrared airglow: A signature of small-scale dynamical processes in the upper atmosphere. Icarus, 2014, 236, 92-103.	1.1	11
107	Open flux in Saturn's magnetosphere. Icarus, 2014, 231, 137-145.	1.1	43
108	Mapping the electron energy in Jupiter's aurora: Hubble spectral observations. Journal of Geophysical Research: Space Physics, 2014, 119, 9072-9088.	0.8	47

#	Article	IF	CITATIONS
109	The Ultraviolet Spectrograph on NASA's Juno Mission. , 2014, , 325-351.		2
110	Hubble observations of Jupiter's north–south conjugate ultraviolet aurora. Icarus, 2013, 226, 1559-1567.	1.1	20
111	Evolution of the Io footprint brightness I: Far-UV observations. Planetary and Space Science, 2013, 88, 64-75.	0.9	32
112	Venus nitric oxide nightglow mapping from SPICAV nadir observations. Icarus, 2013, 226, 428-436.	1.1	35
113	Effects of methane on giant planet's UV emissions and implications for the auroral characteristics. Journal of Molecular Spectroscopy, 2013, 291, 108-117.	0.4	24
114	The characteristics of the O2 Herzberg II and Chamberlain bands observed with VIRTIS/Venus Express. Icarus, 2013, 223, 609-614.	1.1	31
115	Oxygen nightglow emissions of Venus: Vertical distribution and collisional quenching. Icarus, 2013, 223, 602-608.	1.1	13
116	Comparative analysis of airglow emissions in terrestrial planets, observed with VIRTIS-M instruments on board Rosetta and Venus Express. Icarus, 2013, 226, 1115-1127.	1.1	11
117	Evolution of the Io footprint brightness II: Modeling. Planetary and Space Science, 2013, 88, 76-85.	0.9	23
118	Remote sensing of the energy of auroral electrons in Saturn's atmosphere: Hubble and Cassini spectral observations. Icarus, 2013, 223, 211-221.	1.1	11
119	Signatures of magnetospheric injections in Saturn's aurora. Journal of Geophysical Research: Space Physics, 2013, 118, 1922-1933.	0.8	32
120	He ²⁺ transport in the Martian upper atmosphere with an induced magnetic field. Journal of Geophysical Research: Space Physics, 2013, 118, 1231-1242.	0.8	8
121	The multiple spots of the Ganymede auroral footprint. Geophysical Research Letters, 2013, 40, 4977-4981.	1.5	31
122	Auroral signatures of multiple magnetopause reconnection at Saturn. Geophysical Research Letters, 2013, 40, 4498-4502.	1.5	50
123	Jupiter's aurora in ultraviolet and infrared: Simultaneous observations with the Hubble Space Telescope and the NASA Infrared Telescope Facility. Journal of Geophysical Research: Space Physics, 2013, 118, 2286-2295.	0.8	24
124	The OH Venus nightglow spectrum: Intensity and vibrational composition from VIRTIS—Venus Express observations. Planetary and Space Science, 2012, 73, 387-396.	0.9	32
125	Cassini-UVIS observation of dayglow FUV emissions of carbon in the thermosphere of Venus. Icarus, 2012, 220, 635-646.	1.1	29
126	The vertical distribution of the Venus NO nightglow: Limb profiles inversion and one-dimensional modeling. Icarus, 2012, 220, 981-989.	1.1	13

#	Article	IF	CITATIONS
127	Auroral evidence of Io's control over the magnetosphere of Jupiter. Geophysical Research Letters, 2012, 39, .	1.5	111
128	Conversion from HST ACS and STIS auroral counts into brightness, precipitated power, and radiated power for H ₂ giant planets. Journal of Geophysical Research, 2012, 117, .	3.3	60
129	Atomic oxygen on the Venus nightside: Global distribution deduced from airglow mapping. Icarus, 2012, 217, 849-855.	1.1	50
130	Atomic oxygen distributions in the Venus thermosphere: Comparisons between Venus Express observations and global model simulations. Icarus, 2012, 217, 759-766.	1.1	30
131	Spatial correlation of OH Meinel and O2 infrared atmospheric nightglow emissions observed with VIRTIS-M on board Venus Express. Icarus, 2012, 217, 813-817.	1.1	30
132	Quasi-periodic polar flares at Jupiter: A signature of pulsed dayside reconnections?. Geophysical Research Letters, 2011, 38, n/a-n/a.	1.5	53
133	Nightside reconnection at Jupiter: Auroral and magnetic field observations from 26 July 1998. Journal of Geophysical Research, 2011, 116, .	3.3	43
134	Bifurcations of the main auroral ring at Saturn: ionospheric signatures of consecutive reconnection events at the magnetopause. Journal of Geophysical Research, 2011, 116, n/a-n/a.	3.3	69
135	Small-scale structures in Saturn's ultraviolet aurora. Journal of Geophysical Research, 2011, 116, n/a-n/a.	3.3	55
136	Proton and hydrogen atom transport in the Martian upper atmosphere with an induced magnetic field. Journal of Geophysical Research, 2011, 116, n/a-n/a.	3.3	35
137	<i>HUBBLE SPACE TELESCOPE</i> /ADVANCED CAMERA FOR SURVEYS OBSERVATIONS OF EUROPA'S ATMOSPHERIC ULTRAVIOLET EMISSION AT EASTERN ELONGATION. Astrophysical Journal, 2011, 738, 153.	1.6	34
138	The auroral footprint of Enceladus on Saturn. Nature, 2011, 472, 331-333.	13.7	82
139	Measurements of the helium 584Ã airglow during the Cassini flyby of Venus. Planetary and Space Science, 2011, 59, 1524-1528.	0.9	23
140	A layer of ozone detected in the nightside upper atmosphere of Venus. Icarus, 2011, 216, 82-85.	1.1	81
141	EUV spectroscopy of the Venus dayglow with UVIS on Cassini. Icarus, 2011, 211, 70-80.	1.1	47
142	Two-dimensional time-dependent model of the transport of minor species in the Venus night side upper atmosphere. Planetary and Space Science, 2010, 58, 1857-1867.	0.9	10
143	The distributions of the OH Meinel and nightglow emissions in the Venus mesosphere based on VIRTIS observations. Advances in Space Research, 2010, 45, 1268-1275.	1.2	26
144	UVIS observations of the FUV OI and CO 4P Venus dayglow during the Cassini flyby. Icarus, 2010, 207, 549-557.	1.1	47

#	Article	IF	CITATIONS
145	Characteristics of Saturn's FUV airglow from limb-viewing spectra obtained with Cassini-UVIS. Icarus, 2010, 210, 270-283.	1.1	12
146	Comparison of the open-closed field line boundary location inferred using IMAGE-FUV SI12 images and EISCAT radar observations. Annales Geophysicae, 2010, 28, 883-892.	0.6	20
147	Location and spatial shape of electron beams in Io's wake. Journal of Geophysical Research, 2010, 115, .	3.3	29
148	Auroral signatures of flow bursts released during magnetotail reconnection at Jupiter. Journal of Geophysical Research, 2010, 115, .	3.3	32
149	On the origin of Saturn's outer auroral emission. Journal of Geophysical Research, 2010, 115, .	3.3	44
150	Mars ultraviolet dayglow variability: SPICAM observations and comparison with airglow model. Journal of Geophysical Research, 2010, 115, .	3.3	23
151	Venus OH nightglow distribution based on VIRTIS limb observations from Venus Express. Geophysical Research Letters, 2010, 37, .	1.5	19
152	Variation of Saturn's UV aurora with SKR phase. Geophysical Research Letters, 2010, 37, .	1.5	57
153	Atomic oxygen distribution in the Venus mesosphere from observations of O2 infrared airglow by VIRTIS-Venus Express. Icarus, 2009, 199, 264-272.	1.1	27
154	Characteristics of Saturn's polar atmosphere and auroral electrons derived from HST/STIS, FUSE and Cassini/UVIS spectra. Icarus, 2009, 200, 176-187.	1.1	51
155	Recurrent energization of plasma in the midnight-to-dawn quadrant of Saturn's magnetosphere, and its relationship to auroral UV and radio emissions. Planetary and Space Science, 2009, 57, 1732-1742.	0.9	140
156	Venus express: Highlights of the nominal mission. Solar System Research, 2009, 43, 185-209.	0.3	24
157	Observations of Jovian polar auroral filaments. Geophysical Research Letters, 2009, 36, .	1.5	37
158	Equatorward diffuse auroral emissions at Jupiter: Simultaneous HST and Galileo observations. Geophysical Research Letters, 2009, 36, .	1.5	40
159	Saturn's equinoctial auroras. Geophysical Research Letters, 2009, 36, .	1.5	37
160	Variation of different components of Jupiter's auroral emission. Journal of Geophysical Research, 2009, 114, .	3.3	95
161	Auroral footprint of Ganymede. Journal of Geophysical Research, 2009, 114, .	3.3	44
162	The Io UV footprint: Location, interâ€spot distances and tail vertical extent. Journal of Geophysical Research, 2009, 114, .	3.3	77

#	Article	IF	CITATIONS
163	Concurrent observations of the ultraviolet nitric oxide and infrared O ₂ nightglow emissions with Venus Express. Journal of Geophysical Research, 2009, 114, .	3.3	25
164	Altitude of Saturn's aurora and its implications for the characteristic energy of precipitated electrons. Geophysical Research Letters, 2009, 36, .	1.5	81
165	Contributions of the driven process and the loadingâ€unloading process during substorms: A study based on the IMAGEâ€SI12 imager. Journal of Geophysical Research, 2009, 114, .	3.3	3
166	Transient auroral features at Saturn: Signatures of energetic particle injections in the magnetosphere. Journal of Geophysical Research, 2009, 114, .	3.3	35
167	Response of Jupiter's and Saturn's auroral activity to the solar wind. Journal of Geophysical Research, 2009, 114, .	3.3	161
168	The Venus ultraviolet oxygen dayglow and aurora: Model comparison with observations. Planetary and Space Science, 2008, 56, 542-552.	0.9	26
169	Distribution of the O ₂ infrared nightglow observed with VIRTIS on board Venus Express. Geophysical Research Letters, 2008, 35, .	1.5	50
170	UV Io footprint leading spot: A key feature for understanding the UV Io footprint multiplicity?. Geophysical Research Letters, 2008, 35, .	1.5	84
171	Auroral polar dawn spots: Signatures of internally driven reconnection processes at Jupiter's magnetotail. Geophysical Research Letters, 2008, 35, .	1.5	53
172	Jupiterâ \in ™s changing auroral location. Journal of Geophysical Research, 2008, 113, .	3.3	41
173	Discontinuity in Jupiter's main auroral oval. Journal of Geophysical Research, 2008, 113, .	3.3	52
174	Monte Carlo model of electron transport for the calculation of Mars dayglow emissions. Journal of Geophysical Research, 2008, 113, .	3.3	68
175	Distribution of the ultraviolet nitric oxide Martian night airglow: Observations from Mars Express and comparisons with a oneâ€dimensional model. Journal of Geophysical Research, 2008, 113, .	3.3	59
176	Open magnetic flux and magnetic flux closure during sawtooth events. Geophysical Research Letters, 2008, 35, .	1.5	14
177	Auroral evidence of a localized magnetic anomaly in Jupiter's northern hemisphere. Journal of Geophysical Research, 2008, 113, .	3.3	89
178	Origin of Saturn's aurora: Simultaneous observations by Cassini and the Hubble Space Telescope. Journal of Geophysical Research, 2008, 113, .	3.3	127
179	Oscillation of Saturn's southern auroral oval. Journal of Geophysical Research, 2008, 113, .	3.3	88
180	Limb observations of the ultraviolet nitric oxide nightglow with SPICAV on board Venus Express. Journal of Geophysical Research, 2008, 113, .	3.3	55

#	Article	IF	CITATIONS
181	Morphology and dynamics of Venus oxygen airglow from Venus Express/Visible and Infrared Thermal Imaging Spectrometer observations. Journal of Geophysical Research, 2008, 113, .	3.3	52
182	Auroral current systems in Saturn's magnetosphere: comparison of theoretical models with Cassini and HST observations. Annales Geophysicae, 2008, 26, 2613-2630.	0.6	60
183	First detection of hydroxyl in the atmosphere of Venus. Astronomy and Astrophysics, 2008, 483, L29-L33.	2.1	86
184	Clobal morphology of substorm growth phases observed by the IMAGEâ \in SI12 imager. Journal of Geophysical Research, 2007, 112, .	3.3	12
185	Ultraviolet Io footprint short timescale dynamics. Geophysical Research Letters, 2007, 34, .	1.5	20
186	Response of Jupiter's UV auroras to interplanetary conditions as observed by the Hubble Space Telescope during the Cassini flyby campaign. Journal of Geophysical Research, 2007, 112, n/a-n/a.	3.3	66
187	EL - a possible indicator to monitor the magnetic field stretching at global scale during substorm expansive phase: Statistical study. Journal of Geophysical Research, 2007, 112, n/a-n/a.	3.3	14
188	SPICAV on Venus Express: Three spectrometers to study the global structure and composition of the Venus atmosphere. Planetary and Space Science, 2007, 55, 1673-1700.	0.9	160
189	A warm layer in Venus' cryosphere and high-altitude measurements of HF, HCl, H2O and HDO. Nature, 2007, 450, 646-649.	13.7	161
190	A dynamic upper atmosphere of Venus as revealed by VIRTIS on Venus Express. Nature, 2007, 450, 641-645.	13.7	95
191	Europa's FUV auroral tail on Jupiter. Geophysical Research Letters, 2006, 33, .	1.5	29
192	Dayside and nightside reconnection rates inferred from IMAGE FUV and Super Dual Auroral Radar Network data. Journal of Geophysical Research, 2006, 111, .	3.3	71
193	Global auroral proton precipitation observed by IMAGE-FUV: Noon and midnight brightness dependence on solar wind characteristics and IMF orientation. Journal of Geophysical Research, 2006, 111, .	3.3	9
194	Morphology of the ultraviolet Io footprint emission and its control by Io's location. Journal of Geophysical Research, 2006, 111, .	3.3	50
195	Compression of the Earth's magnetotail by interplanetary shocks directly drives transient magnetic flux closure. Geophysical Research Letters, 2006, 33, n/a-n/a.	1.5	40
196	Characteristics of Jovian morning bright FUV aurora from Hubble Space Telescope/Space Telescope Imaging Spectrograph imaging and spectral observations. Journal of Geophysical Research, 2006, 111, .	3.3	48
197	Energetic oxygen atoms in the polar geocorona. Journal of Geophysical Research, 2006, 111, .	3.3	9
198	Saturn's auroral morphology and activity during quiet magnetospheric conditions. Journal of Geophysical Research, 2006, 111, .	3.3	35

#	Article	IF	CITATIONS
199	A statistical analysis of the location and width of Saturn's southern auroras. Annales Geophysicae, 2006, 24, 3533-3545.	0.6	82
200	A View to the Future: Ultraviolet Studies of the Solar System. Astrophysics and Space Science, 2006, 303, 103-122.	0.5	3
201	The Cassini Campaign observations of the Jupiter aurora by the Ultraviolet Imaging Spectrograph and the Space Telescope Imaging Spectrograph. Icarus, 2005, 178, 327-345.	1.1	23
202	Statistical properties of dayside subauroral proton flashes observed with IMAGE-FUV. Geophysical Monograph Series, 2005, , 195-205.	0.1	2
203	Morphological differences between Saturn's ultraviolet aurorae and those of Earth and Jupiter. Nature, 2005, 433, 717-719.	13.7	155
204	Solar wind dynamic pressure and electric field as the main factors controlling Saturn's aurorae. Nature, 2005, 433, 720-722.	13.7	126
205	A Monte Carlo model of auroral hydrogen emission line profiles. Annales Geophysicae, 2005, 23, 1473-1480.	0.6	5
206	An Earth-like correspondence between Saturn's auroral features and radio emission. Nature, 2005, 433, 722-725.	13.7	104
207	An auroral source of hot oxygen in the geocorona. Geophysical Research Letters, 2005, 32, .	1.5	12
208	Reconnection in a rotation-dominated magnetosphere and its relation to Saturn's auroral dynamics. Journal of Geophysical Research, 2005, 110, .	3.3	151
209	Comparison of intense nightside shock-induced precipitation and substorm activity. Journal of Geophysical Research, 2005, 110, .	3.3	19
210	Variable morphology of Saturn's southern ultraviolet aurora. Journal of Geophysical Research, 2005, 110, .	3.3	96
211	Signature of Saturn's auroral cusp: Simultaneous Hubble Space Telescope FUV observations and upstream solar wind monitoring. Journal of Geophysical Research, 2005, 110, .	3.3	52
212	Far ultraviolet remote sensing of the isotropy boundary and magnetotail stretching. Journal of Geophysical Research, 2005, 110, .	3.3	12
213	Open flux estimates in Saturn's magnetosphere during the January 2004 Cassini-HST campaign, and implications for reconnection rates. Journal of Geophysical Research, 2005, 110, .	3.3	92
214	Global auroral conductance distribution due to electron and proton precipitation from IMAGE-FUV observations. Annales Geophysicae, 2004, 22, 1595-1611.	0.6	27
215	Study of the vertical structure of Saturn's atmosphere using HST/WFPC2 images. Icarus, 2004, 169, 413-428.	1.1	22
216	Jovian auroral spectroscopy with FUSE: analysis of self-absorption and implications for electron precipitation. Icarus, 2004, 171, 336-355.	1.1	39

#	Article	IF	CITATIONS
217	DYNAMO: a Mars upper atmosphere package for investigating solar wind interaction and escape processes, and mapping Martian fields. Advances in Space Research, 2004, 33, 2228-2235.	1.2	3
218	Solar wind control of auroral substorm onset locations observed with the IMAGE-FUV imagers. Journal of Geophysical Research, 2004, 109, .	3.3	30
219	Proton precipitation during transpolar auroral events: Observations with the IMAGE-FUV imagers. Journal of Geophysical Research, 2004, 109, .	3.3	11
220	A possible auroral signature of a magnetotail reconnection process on Jupiter. Journal of Geophysical Research, 2004, 109, .	3.3	64
221	Morphology and seasonal variations of global auroral proton precipitation observed by IMAGE-FUV. Journal of Geophysical Research, 2004, 109, .	3.3	17
222	Energy-flux relationship in the FUV Jovian aurora deduced from HST-STIS spectral observations. Journal of Geophysical Research, 2004, 109, .	3.3	55
223	Propagation of electron and proton shock-induced aurora and the role of the interplanetary magnetic field and solar wind. Journal of Geophysical Research, 2004, 109, .	3.3	51
224	Characteristics of Saturn's FUV aurora observed with the Space Telescope Imaging Spectrograph. Journal of Geophysical Research, 2004, 109, .	3.3	84
225	Global Imaging of Proton and Electron Aurorae in the far Ultraviolet. Space Science Reviews, 2003, 109, 211-254.	3.7	17
226	Summary of quantitative interpretation of IMAGE far ultraviolet auroral data. Space Science Reviews, 2003, 109, 255-283.	3.7	60
227	Observation of dayside subauroral proton flashes with the IMAGE-FUV imagers. Geophysical Research Letters, 2003, 30, .	1.5	49
228	IMAGE FUV and in situ FAST particle observations of substorm aurorae. Journal of Geophysical Research, 2003, 108, .	3.3	42
229	Characterization and dynamics of the auroral electron precipitation during substorms deduced from IMAGE-FUV. Journal of Geophysical Research, 2003, 108, .	3.3	13
230	Dynamics of global scale electron and proton precipitation induced by a solar wind pressure pulse. Geophysical Research Letters, 2003, 30, .	1.5	35
231	Spectral observations of transient features in the FUV Jovian polar aurora. Journal of Geophysical Research, 2003, 108, .	3.3	35
232	Jupiter's polar auroral emissions. Journal of Geophysical Research, 2003, 108, .	3.3	135
233	Remote sensing of the proton aurora characteristics from IMACE-FUV. Annales Geophysicae, 2003, 21, 2165-2173.	0.6	8
234	Summary of Quantitative Interpretation of IMAGE Far Ultraviolet Auroral Data. , 2003, , 255-283.		1

Summary of Quantitative Interpretation of IMAGE Far Ultraviolet Auroral Data. , 2003, , 255-283. 234

14

#	Article	IF	CITATIONS
235	Global Imaging of Proton and Electron Aurorae in the Far Ultraviolet. , 2003, , 211-254.		О
236	Interplanetary magnetic field control of afternoon-sector detached proton auroral arcs. Journal of Geophysical Research, 2002, 107, SMP 17-1.	3.3	52
237	Total electron and proton energy input during auroral substorms: Remote sensing with IMAGE-FUV. Journal of Geophysical Research, 2002, 107, SMP 15-1-SMP 15-12.	3.3	40
238	Electron and proton excitation of the FUV aurora: Simultaneous IMAGE and NOAA observations. Journal of Geophysical Research, 2002, 107, SIA 5-1.	3.3	32
239	Proton aurora in the cusp. Journal of Geophysical Research, 2002, 107, SMP 2-1.	3.3	115
240	Excitation of the FUV Io tail on Jupiter: Characterization of the electron precipitation. Journal of Geophysical Research, 2002, 107, SMP 30-1.	3.3	59
241	IMAGE and FAST observations of substorm recovery phase aurora. Geophysical Research Letters, 2002, 29, 43-1.	1.5	12
242	Global comparison of magnetospheric ion fluxes and auroral precipitation during a substorm. Geophysical Research Letters, 2002, 29, 51-1.	1.5	18
243	Spatially Resolved Far Ultraviolet Spectroscopy of the Jovian Aurora. Icarus, 2002, 157, 91-103.	1.1	25
244	Ultraviolet emissions from the magnetic footprints of Io, Ganymede and Europa on Jupiter. Nature, 2002, 415, 997-1000.	13.7	203
245	Observation of the proton aurora with IMAGE FUV imager and simultaneous ion flux in situ measurements. Journal of Geophysical Research, 2001, 106, 28939-28948.	3.3	58
246	Global observations of proton and electron auroras in a substorm. Geophysical Research Letters, 2001, 28, 1139-1142.	1.5	40
247	The electron and proton aurora as seen by IMAGE-FUV and FAST. Geophysical Research Letters, 2001, 28, 1135-1138.	1.5	61
248	Ion outflow observed by IMAGE: Implications for source regions and heating mechanisms. Geophysical Research Letters, 2001, 28, 1163-1166.	1.5	50
249	The role of proton precipitation in the excitation of auroral FUV emissions. Journal of Geophysical Research, 2001, 106, 21475-21494.	3.3	35
250	Observation of anomalous temperatures in the daytime O(1D) 6300 Ã thermospheric emission: A possible signature of nonthermal atoms. Journal of Geophysical Research, 2001, 106, 12753-12764.	3.3	15
251	A self-consistent model of the Jovian auroral thermal structure. Journal of Geophysical Research, 2001, 106, 12933-12952.	3.3	169
252	Modelling short-term CO2 fluxes and long-term tree growth in temperate forests with ASPECTS. Ecological Modelling, 2001, 141, 35-52.	1.2	42

#	Article	IF	CITATIONS
253	Diagnostics of the Jovian Aurora Deduced from Ultraviolet Spectroscopy: Model and HST/GHRS Observations. Icarus, 2000, 147, 251-266.	1.1	38
254	Far ultraviolet imaging from the IMAGE spacecraft. 1. System design. Space Science Reviews, 2000, 91, 243-270.	3.7	211
255	Far ultraviolet imaging from the IMAGE spacecraft. 3. Spectral imaging of Lyman-α and OI 135.6 nm. Space Science Reviews, 2000, 91, 287-318.	3.7	194
256	A model of the Lyman-α line profile in the proton aurora. Journal of Geophysical Research, 2000, 105, 15795-15805.	3.3	65
257	Far Ultraviolet Imaging from the Image Spacecraft. 3. Spectral Imaging of Lyman-â^•and OI 135.6 nm. , 2000, , 287-318.		8
258	Comparing global models of terrestrial net primary productivity (NPP): analysis of the seasonal atmospheric CO 2 signal. Global Change Biology, 1999, 5, 65-76.	4.2	31
259	Thermalization of O(1D) atoms in the thermosphere. Journal of Geophysical Research, 1999, 104, 4287-4295.	3.3	45
260	The interannual change of atmospheric CO2: Contribution of subtropical ecosystems?. Geophysical Research Letters, 1999, 26, 243-246.	1.5	38
261	Effect of hot oxygen on thermospheric O I UV airglow. Journal of Geophysical Research, 1999, 104, 17139-17143.	3.3	10
262	The Longitudinal Variation of the Color Ratio of the Jovian Ultraviolet Aurora: A Geometric Effect?. Geophysical Research Letters, 1998, 25, 1601-1604.	1.5	7
263	Hubble Space Telescope imaging of Jupiter's UV aurora during the Galileo orbiter mission. Journal of Geophysical Research, 1998, 103, 20217-20236.	3.3	170
264	HSTSpectra of the Jovian Ultraviolet Aurora: Search for Heavy Ion Precipitation. Astrophysical Journal, 1998, 507, 955-967.	1.6	24
265	An updated model of the hot nitrogen atom kinetics and thermospheric nitric oxide. Journal of Geophysical Research, 1997, 102, 285-294.	3.3	36
266	Simulation of the Morphology of the Jovian UV North Aurora Observed with the Hubble Space Telescope. Icarus, 1997, 128, 306-321.	1.1	23
267	The seasonality of the CO2exchange between the atmosphere and the land biosphere: A study with a global mechanistic vegetation model. Journal of Geophysical Research, 1996, 101, 7111-7125.	3.3	39
268	The equatorial boundary of the ultraviolet Jovian north aurora observed with multispectral Hubble Space Telescope images. Journal of Geophysical Research, 1996, 101, 2163-2168.	3.3	7
269	High rotational excitation of NO infrared thermospheric airglow: A signature of superthermal nitrogen atoms?. Geophysical Research Letters, 1996, 23, 2215-2218.	1.5	11
270	The distribution of hot hydrogen atoms produced by electron and proton precipitation in the Jovian aurora. Journal of Geophysical Research, 1996, 101, 21157-21168.	3.3	17

#	Article	IF	CITATIONS
271	Seasonal and interannual influences of the terrestrial ecosystems on atmospheric CO2: a model study. Physics and Chemistry of the Earth, 1996, 21, 537-544.	0.3	2
272	HST far-ultraviolet imaging of Jupiter during the impacts of comet Shoemaker-Levy 9. Science, 1995, 267, 1302-1307.	6.0	64
273	The importance of new chemical sources for the hot oxygen geocorona. Geophysical Research Letters, 1995, 22, 279-282.	1.5	22
274	Auroral Lyman α and H2bands from the giant planets: 2. Effect of the anisotropy of the precipitating particles on the interpretation of the "color ratio― Journal of Geophysical Research, 1995, 100, 7513.	3.3	13
275	Simultaneous observations of the Saturnian aurora and polar haze with the HST/FOC. Geophysical Research Letters, 1995, 22, 2685-2688.	1.5	44
276	The morphology of the north Jovian ultraviolet aurora observed with the Hubble Space Telescope. Planetary and Space Science, 1994, 42, 905-917.	0.9	48
277	Auroral Lyman α and H2bands from the giant planets: 1. Excitation by proton precipitation in the Jovian atmosphere. Journal of Geophysical Research, 1994, 99, 17075.	3.3	48
278	CARAIB: A global model of terrestrial biological productivity. Global Biogeochemical Cycles, 1994, 8, 255-270.	1.9	165
279	A kinetic model of the formation of the hot oxygen geocorona: 1. Quiet geomagnetic conditions. Journal of Geophysical Research, 1994, 99, 23217.	3.3	88
280	A Remarkable Auroral Event on Jupiter Observed in the Ultraviolet with the Hubble Space Telescope. Science, 1994, 266, 1675-1678.	6.0	55
281	High-resolution spectra of Jupiter's northern auroral ultraviolet emission with the Hubble Space Telescope. Astrophysical Journal, 1994, 421, 816.	1.6	50
282	Hubble Space Telescope Goddard high-resolution spectrograph H2 rotational spectra of Jupiter's aurora. Astrophysical Journal, 1994, 430, L73.	1.6	41
283	A first look at the ASSI ultraviolet results. Advances in Space Research, 1993, 13, 247-254.	1.2	1
284	Morphology and time variation of the Jovian far UV aurora: Hubble space telescope observations. Journal of Geophysical Research, 1993, 98, 18793-18801.	3.3	38
285	A sensitivity study of the role of continental location and area on Paleozoic climate. Global and Planetary Change, 1992, 5, 311-323.	1.6	2
286	The faint young sun climatic paradox: A simulation with an interactive seasonal climate-sea ice model. Global and Planetary Change, 1992, 5, 133-150.	1.6	6
287	Ultraviolet imaging of the Jovian aurora with the Hubble Space Telescope. Geophysical Research Letters, 1992, 19, 1803-1806.	1.5	53
288	The faint young sun climatic paradox: A simulation with an interactive seasonal climate-sea ice model. Palaeogeography, Palaeoclimatology, Palaeoecology, 1992, 97, 133-150.	1.0	14

#	Article	IF	CITATIONS
289	A sensitivity study of the role of continental location and area on Paleozoic climate. Palaeogeography, Palaeoclimatology, Palaeoecology, 1992, 97, 311-323.	1.0	0
290	Thermospheric odd nitrogen. Planetary and Space Science, 1992, 40, 337-353.	0.9	30
291	Non thermal nitrogen atoms in the Earth's thermosphere 1. Kinetics of hot N(⁴ S). Geophysical Research Letters, 1991, 18, 1691-1694.	1.5	31
292	Non thermal nitrogen atoms in the Earth's thermosphere 2. A source of nitric oxide. Geophysical Research Letters, 1991, 18, 1695-1698.	1.5	33
293	The diurnal variation of NO, N(\hat{A}^2D), and ions in the thermosphere: A comparison of satellite measurements to a model. Journal of Geophysical Research, 1991, 96, 11331-11339.	3.3	28
294	The warm Cretaceous climate: Role of the longâ€ŧerm carbon cycle. Geophysical Research Letters, 1990, 17, 1561-1564.	1.5	6
295	The Venus nitric oxide night airglow: Model calculations based on the Venus thermospheric general circulation model. Journal of Geophysical Research, 1990, 95, 6271-6284.	3.3	88
296	The latitudinal gradient of the NO peak density. Journal of Geophysical Research, 1990, 95, 19053-19059.	3.3	16
297	The maximum entropy production principle in climate models: Application to the faint young sun paradox. Quarterly Journal of the Royal Meteorological Society, 1990, 116, 1123-1132.	1.0	21
298	Rapid deactivation of N(² <i>D</i>) by O: Impact on thermospheric and mesospheric odd nitrogen. Journal of Geophysical Research, 1989, 94, 5419-5426.	3.3	27
299	Sources and distribution of odd nitrogen in the Venus daytime thermosphere. Icarus, 1988, 75, 171-184.	1.1	13
300	Ozone, climate and biospheric environment in the ancient oxygen-poor atmosphere. Planetary and Space Science, 1988, 36, 1391-1414.	0.9	15
301	The role of nitric oxide on the zonally averaged structure of the thermosphere: Solstice conditions for solar cycle maximum. Planetary and Space Science, 1988, 36, 271-279.	0.9	15
302	AEâ€Ð measurements of the NO geomagnetic latitudinal distribution and contamination by N ⁺ (⁵ <i>S</i>) emission. Journal of Geophysical Research, 1986, 91, 10136-10140.	3.3	18
303	Reducing power of ferrous iron in the Archean Ocean, 1. Contribution of photosynthetic oxygen. Paleoceanography, 1986, 1, 355-368.	3.0	11
304	A numerical model of the evolution of ocean sulfate and sedimentary sulfur during the last 800 million years. Geochimica Et Cosmochimica Acta, 1986, 50, 2289-2302.	1.6	32
305	The role of nitric oxide on the zonally averaged structure of the thermosphere: Solstice conditions for solar cycle minimum. Planetary and Space Science, 1986, 34, 131-144.	0.9	16
306	The E-region electron density diurnal asymmetry at Saint-Santin: observations and role of nitric oxide. Journal of Atmospheric and Solar-Terrestrial Physics, 1986, 48, 471-483.	0.9	14

#	Article	IF	CITATIONS
307	The global distribution of thermospheric odd nitrogen for solstice conditions during solar cycle minimum. Journal of Geophysical Research, 1984, 89, 1725-1738.	3.3	36
308	The thermospheric heating efficiency under electron precipitation conditions. Planetary and Space Science, 1982, 30, 1083-1089.	0.9	13
309	Transport of aurorally produced N(2D) by winds in the high latitude thermosphere. Planetary and Space Science, 1982, 30, 1091-1105.	0.9	21
310	The altitude distribution of the Venus ultraviolet nightglow and implications on vertical transport. Geophysical Research Letters, 1981, 8, 633-636.	1.5	39
311	The effect of particle precipitation events on the neutral and ion chemistry of the middle atmosphere—1. Odd nitrogen. Planetary and Space Science, 1981, 29, 767-774.	0.9	185
312	The effect of particle precipitation events on the neutral and ion chemistry of the middle atmosphere: II. Odd hydrogen. Planetary and Space Science, 1981, 29, 885-893.	0.9	257
313	Satellite studies of N(²D) emission and ion chemistry in aurorae. Journal of Geophysical Research, 1980, 85, 1285-1290.	3.3	33
314	Metastable N(\hat{A}^2 <i>P</i>) atoms in the aurora. Journal of Geophysical Research, 1980, 85, 1757-1761.	3.3	13
315	Morphology of the Venus ultraviolet night airglow. Journal of Geophysical Research, 1980, 85, 7861-7870.	3.3	113
316	The auroral ionosphere: Comparison of a timeâ€dependent model with composition measurements. Journal of Geophysical Research, 1979, 84, 4335-4340.	3.3	33
317	The reaction of N(²D) with O ₂ as a source of O (¹D) atoms in aurorae. Geophysical Research Letters, 1978, 5, 1043-1046.	1.5	55
318	The Mg II equatorial airglow altitude distribution. Journal of Geophysical Research, 1978, 83, 4389-4391.	3.3	23
319	Rocket and ground-based measurements of the dayside magnetospheric cleft from Cape Parry, N.W.T Geophysical Research Letters, 1976, 3, 69-72.	1.5	23
320	Rocket-borne baffled photometer: design and calibration. Applied Optics, 1976, 15, 437.	2.1	5
321	OGO-4 observations of the ultraviolet auroral spectrum. Planetary and Space Science, 1976, 24, 1059-1063.	0.9	25
322	Photometric measurements of the O2 U.V. nightglow. Planetary and Space Science, 1975, 23, 1681-1684.	0.9	10
323	Satellite observations of the nitric oxide nightglow. Geophysical Research Letters, 1975, 2, 179-182.	1.5	25
324	Ultraviolet observations of equatorial dayglow above the <i>F</i> ₂ peak. Journal of Geophysical Research, 1973, 78, 4641-4650.	3.3	56

#	Article	IF	CITATIONS
325	Secondary electron excitation in the aurora. Journal of Atmospheric and Solar-Terrestrial Physics, 1972, 34, 531-535.	0.9	5
326	Aeronomy and Paleoclimate. Geophysical Monograph Series, 0, , 139-148.	0.1	3
327	The Role of Fast N(⁴ S) Atoms and Energetic Photoelectrons on the Distribution of NO in the Thermosphere. Geophysical Monograph Series, 0, , 235-241.	0.1	6